Plant Physiol. (1995) 109: 319–326

Kinetics of NO_3^- Influx in Spruce[1]

Herbert J. Kronzucker, M. Yaeesh Siddiqi, and Anthony D. M. Glass*
Department of Botany, University of British Columbia, Vancouver, British Columbia, Canada V6T 1Z4

Influxes of $^{13}NO_3^-$ across the root plasmalemma were measured in intact seedlings of *Picea glauca* (Moench) Voss. Three kinetically distinct uptake systems for NO_3^- were identified. In seedlings not previously exposed to external NO_3^-, a single Michaelis-Menten-type constitutive high-affinity transport system (CHATS) operated in a 2.5 to 500 µM range of external NO_3^- $[NO_3^-]_o$. The V_{max} of this system was 0.1 µmol g^{-1} h^{-1}, and the K_m was approximately 15 µM. Following exposure to NO_3^- for 3 d, this CHATS activity was increased approximately 3-fold, with no change of K_m. In addition, a NO_3^--inducible high-affinity system became apparent with a K_m of approximately 100 µM. The combined V_{max} for these discrete saturable components was 0.7 µmol g^{-1} h^{-1}. In both uninduced and induced plants a linear low-affinity system, additive to CHATS and an NO_3^--inducible high-affinity system, operated at $[NO_3^-]_o \geq 1$ mM. The time taken to achieve maximal rates of uptake (full induction) was 2 d from 1.5 mM $[NO_3^-]_o$ and 3 d from 200 µM $[NO_3^-]_o$.

NO_3^- uptake in higher plants is well characterized on the kinetics level (Clarkson, 1986). There is general agreement in the literature that the dependence of NO_3^- uptake on $[NO_3^-]_o$ can be resolved into at least two kinetically distinct systems (Clarkson and Lüttge, 1991; Glass and Siddiqi, 1995). Most kinetic experiments on NO_3^- uptake have been performed in cereal species and have been based on measurements of chemical depletion rates of NO_3^- from nutrient solutions, i.e. the determination of NO_3^- net flux (Neyra and Hageman, 1976; Rao and Rains, 1976; Doddema and Telkamp, 1979; Breteler and Nissen, 1982; Pace and McClure, 1986; Warner and Huffaker, 1989; Aslam et al., 1992). Although kinetic inferences from net flux studies have to be approached with caution, studies using radiotracers to determine the unidirectional influx of NO_3^- into root tissue have confirmed a (biphasic) pattern for NO_3^- uptake (Siddiqi et al., 1990). In the majority of studies, NO_3^- uptake appeared to be mediated by a HATS, which operated in a Michaelis-Menten-type fashion at $[NO_3^-]_o \leq 1$ mM, and by a LATS, which operated in a linear fashion at $[NO_3^-]_o \geq 1$ mM. Only a few workers reported apparently different or more complex patterns (Doddema and Telkamp, 1979; Breteler and Nissen, 1982).

The NO_3^- uptake system in higher plants is unusual in that it is subject to induction by external NO_3^- (Minotti et al., 1969; see also Kronzucker et al., 1995b, for refs), i.e. NO_3^- influx and net flux are considerably enhanced following initial exposure of roots to solution NO_3^-. Several workers have compared the concentration dependence of NO_3^- uptake in induced and uninduced states. Uninduced plants exhibited a CHATS with saturable kinetics (Lee and Drew, 1986; Behl et al., 1988; Klobus et al., 1988; Siddiqi et al., 1989, 1990; Hole et al., 1990). Because of significant differences in K_m (Lee and Drew, 1986; Warner and Huffaker, 1989; Aslam et al., 1992) and response to metabolic poisons (Jackson et al., 1973), CHATS was considered a genetically discrete system from the IHATS apparent in the induced state (Clarkson, 1986). In some plants, the CHATS and IHATS were found to operate concurrently in the induced state (Warner and Huffaker, 1989; Aslam et al., 1992), whereas in others this was not obvious (Siddiqi et al., 1990).

In contrast to the large body of experimental work on cereal species, our knowledge of NO_3^- uptake kinetics in conifer species is rudimentary, in spite of the enormous ecological and economic importance of such species. Only a small number of NO_3^- depletion studies in conifers have been reported (Peuke and Tischner, 1991; Kamminga-van Wijk and Prins, 1993; Plassard et al., 1994) and have provided no conclusive results as to the identity of the transport systems or their operation at different states of induction. It is possible that the poor growth response of many conifers on soils with NO_3^- as the predominant source of nitrogen (Kronzucker et al., 1995a, 1995b, 1995c) can be attributed to a lower capacity of the NO_3^- transport system in conifers than usually is characteristic of the more-studied cereals. The purpose of the present communication thus is to characterize the kinetics of the NO_3^- uptake system in white spruce (*Picea glauca* [Moench] Voss.). We have used the radiotracer ^{13}N to conduct direct measurements of unidirectional NO_3^- influx as a function of both $[NO_3^-]_o$ and the time of exposure to external NO_3^-.

MATERIALS AND METHODS

Plant Growth Conditions

Seedlings of white spruce (*Picea glauca* [Moench] Voss., provenance 29170, from the Prince George region in British

[1] The work reported in this paper was supported by a National Sciences and Engineering Research Council of Canada grant to A.D.M.G. and by a University of British Columbia Graduate Fellowship to H.J.K.

* Corresponding author; e-mail aglass@unixg.ubc.ca; fax 1-604-822-6089.

Abbreviations: CHATS, constitutive high-affinity transport system; HATS, high-affinity transport system; IHATS, inducible high-affinity transport system; LATS, low-affinity transport system; $[NO_3^-]_o$, external NO_3^- concentration; *v*, used in data transformation equations (of Michaelis-Menten-type data) to indicate the unidirectional influx of NO_3^- at a given value of $[NO_3^-]_o$; V_{max}, maximal unidirectional NO_3^- influx (according to Michaelis-Menten formalism).

Columbia, Canada) were used. Seedlings were grown for a minimum of 3.5 months in a peat:perlite (3:1) mixture in Styrofoam boxes in an outdoor nursery located on the University of British Columbia campus. Seedlings were then transported to indoor growth chambers and, after gentle removal of the rooting medium, transferred to hydroponic culture in 24-L Plexiglas tanks. The tanks contained one-tenth-strength N-free Johnson's solution. A detailed description of growth conditions and exact solution composition was given by Kronzucker et al. (1995a). Seedling roots maintained in hydroponic solution were nonmycorrhizal, as determined by microscopic examination. The seedlings were maintained in the tanks for 3 weeks before influx experiments were conducted. NO_3^- was withheld completely from growth tanks, except in induction experiments, in which NO_3^- was added as $Ca(NO_3)_2$, either at 200 μM or 1.5 mM, at times ranging from 3 h to 7 d prior to influx measurements (see text for details). In concentration dependence experiments in which induced seedlings were used, induction was at 100 μM $[NO_3^-]_o$ for 3 d. Solutions were checked daily for $[K^+]$ using an Instrumentation Laboratory (Lexington, MA) model 443 flame photometer. The pH of solutions was maintained at 6.5 ($\pm$0.3) by addition of powdered $CaCO_3$ to the tanks; pH was monitored daily using a microprocessor-based pocket-size pH meter (pH Testr2 model 59000–20; Cole Parmer, Chicago, IL). $[NO_3^-]_o$ was determined daily following the method by Cawse (1967) and using a Philips PU 8820 UV/VIS spectrophotometer. Solutions were replaced every 4 d. All seedlings were maintained in a 16-h/8-h photoperiod, 70% RH, and at 20 $\pm$ 2°C. A photon flux of approximately 250 μmol m^{-2} s^{-1} measured at plant level (with an LI-189 light meter and LI-190SA quantum sensor from Li-Cor, Lincoln, NE) was provided by fluorescent lamps (VITA-LITE/DURO-TEST, U.S. Patent 3,670,193).

Influx Measurements

The radiotracer ^{13}N (half-life = 9.96 min) was produced by the cyclotron facility (Tri-University Meson Facility) at the University of British Columbia (Vancouver, Canada). Proton irradiation of a water target was used as the isotope generation procedure, which provided $^{13}NO_3^-$ with high radiochemical purity (Kronzucker et al., 1995a). An irradiated solution of approximately 700 to 740 MBq was supplied in sealed 20-mL glass vials. Procedures for the removal of radiocontaminants were as described in detail elsewhere (Kronzucker et al., 1995a, 1995b). Following purification, the $^{13}NO_3^-$ solution was added to a volume of 4 to 6 L of vigorously stirred uptake solution. The nutrient composition of the uptake solution was the same as the hydroponic growth solution. The uptake solution was contained in a double-neck Erlenmeyer flask, which was located on a stir-plate behind lead. The flask was pressurized remotely via a hand-operated pump to deliver the labeled uptake solution to 8 to 12 individual 500-mL uptake vessels. NO_3^- had been added before to these vessels in the form of $Ca(NO_3)_2$ at the desired concentrations, with a range of 2.5 μM to 50 mM (see influx isotherms).

Seedlings were transferred from the hydroponic growth tanks to prewash solutions in 1-L vessels for 5 min prior to immersion of the roots of intact seedlings in the labeled uptake solutions, to minimize perturbation and to equilibrate plant roots to the exact solution temperature and composition used during influx. After the prewash, seedlings were transferred to the uptake vessels for 10 min. Immediately following the 10-min loading, roots were dipped into nonlabeled solutions for 5 s to minimize carryover of label by the root surface to the desorption solution. Roots were then postwashed in nonlabeled solution for 2 min to desorb $^{13}NO_3^-$ contained in the free space.

In earlier compartmental analysis studies of roots of intact white spruce seedlings (Kronzucker et al., 1995a, 1995b) the half-lives of exchange for NO_3^- with the root surface, the cell wall, and the cytoplasm were determined to be approximately 2.5 s, 20 s, and 7 min, respectively. The durations for prewash, labeling, dip, and postwash were selected based on this information. By loading plants in $^{13}NO_3^-$-labeled solution for 10 min, i.e. less than 1.5 half-lives of exchange for the cytoplasmic compartment, and by subsequently desorbing the labeled roots for 2 min, i.e. 4 to 5 half-lives of exchange of the cell wall, any errors introduced by efflux during the loading period or by counts remaining in the cell-wall fraction at the end of the experiment should have been minimized (Cram, 1968).

Following desorption, seedling roots were excised from the shoots, the roots were spun in a low-speed centrifuge for 30 s to remove surface liquid, and the fresh weights of roots and shoots were determined. The plant organs were then stuffed into 20-mL scintillation vials, and the radioactivities of roots and shoots were determined in a Packard γ-counter (Minaxi δ, Auto-γ 5000 series) for measurement of the 511-keV positron-electron annihilation radiation generated by recombination of ambient electrons and β^+ particles emitted from ^{13}N. Using the value for specific activity ($^{13}N/[^{13}N + {}^{14}N]$) of the loading solution and the fresh root weight of each seedling, we calculated NO_3^- fluxes and expressed them in μmol g^{-1} fresh weight h^{-1} (see below).

The root system in the several-month-old spruce seedlings was visibly heterogeneous. Numerous new laterals emerged during the 3-week cultivation period in hydroponic tanks (referred to as "young" roots), which were noticeably different from the root system already existing at the time of transfer. These newly formed roots attained, on average, lengths of 3 to 5 cm and were exclusively of the "white-zone" type (Sutton and Tinus, 1983; McKenzie and Peterson, 1995a), i.e. showed no macroscopic signs of root browning due to either tannin formation or periderm initiation. This white-zone part of the conifer seedling root system is known to largely resemble young roots of herbaceous plants in terms of structure and permeability characteristics (Rüdinger et al., 1994; McKenzie and Peterson, 1995a). By contrast, the part of the root system that was already established at the time of transfer to hydroponics was brown in color (average length: 8–12 cm; referred to as "old" roots). It corresponded to the "tannin zone" and the early-periderm region (McKenzie and Peterson, 1995a, 1995b). Deposition of brown tannins has been causally linked to cortical cell senescence (Sutton and Tinus, 1983), and changes in water and solute permeability characteristics (Kramer, 1969; Rüdinger et al., 1994) and a decline in specific ion uptake capacity (Kamula and Peterson, 1994) have been observed. Similarly, incipient suberin incrustation in the early-periderm region is expected to reduce ion uptake rates.

In our experiments, specific NO_3^- uptake rates by old roots were typically only 20 to 30% of those by young roots (data not shown). In some selected experiments, we have excised labeled roots at the point of transition from the white zone to the tannin/early-periderm zone, which was clearly discernible. This was performed immediately following desorption in postwash solutions. Fresh weights of young and old roots were recorded, and the accumulation of ^{13}N in the excised parts was determined individually. Specific NO_3^- influxes for old, young, or whole roots were then calculated by dividing by the fresh weights of the respective tissues. Unless otherwise indicated, however, integrated influx values, determined on a whole-root basis, were used in figures and tables.

Data Analysis

All experiments were replicated at least three times. Each experimental treatment consisted of three seedling samples (minimum root mass was 3 g fresh weight per sample). Data from several experiments were pooled ($n \geq 9$) for calculations of means and SE. These values were used for plotting representative time induction curves and uptake isotherms as well as for calculating V_{max} and K_m values. Four separate data transformation methods (Cornish-Bowden and Wharton, 1988), based on the Michaelis-Menten formalism, were used to obtain V_{max} and K_m estimates for the saturable isotherm components in the present study. These methods were: (a) linear transformation according to Lineweaver-Burk: $1/v = K_m/V_{max} \cdot 1/[NO_3^-]_o + 1/V_{max}$; (b) linear transformation according to Eadie-Hofstee: $v = V_{max} - K_m \cdot v/[NO_3^-]_o$; (c) linear transformation according to Hanes-Wolf: $[NO_3^-]_o/v = K_m/V_{max} + [NO_3^-]_o/V_{max}$; and (d) least-squares method by Cornish-Bowden: $K_m = (\Sigma v^2 \cdot \Sigma v/[NO3^-]_o - \Sigma v^2/[NO_3^-]_o \cdot \Sigma v)/\Sigma v^2/[NO_3^-]_o^2 \cdot \Sigma v - \Sigma v^2[NO_3^-]_o \Sigma v/[NO_3^-]_o)$; $V_{max} = (\Sigma v^2/[NO_3^-]_o^2 \cdot \Sigma v^2 - (\Sigma v^2/[NO_3^-]_o)^2)/\Sigma v^2/[NO_3^-]_o^2 \cdot \Sigma v - \Sigma v^2/[NO_3^-]_o \cdot \Sigma v/[NO_3^-]_o)$.

Student's t tests were used to examine the slopes and y intercepts of linear transformations for significant differences of regression lines of the two assumed components of the biphasic (i.e. bisaturable) induced HATS.

Estimates of K_m and V_{max} values obtained by the various transformation methods (see "Results") were not identical. Thus, to avoid subjective data representation, no one specific fit was preferred over another for the Michaelis-Menten phases in isotherm plots. Rather, in isotherms (see Fig. 4), data points were connected directly.

RESULTS

Time Profile of Induction of NO_3^- Influx by NO_3^-

Measured NO_3^- influx of N-deprived seedlings was enhanced with increased time of exposure to $[NO_3^-]_o$ for up to 72 h (Figs. 1 and 2). In the uninduced state, influx measured at 200 μM was 0.1 to 0.15 μmol g^{-1} h^{-1}. Peak influx (0.6–0.7 μmol g^{-1} h^{-1}) was reached after 3 d of induction (Fig. 2), after which point influx declined to a value of 0.3 μmol g^{-1} h^{-1} by 7 d. This value at 7 d corresponded to the net flux of NO_3^- measured by chemical depletion under steady-state conditions (data not shown). This time course of NO_3^- influx was evident on a whole-root basis as well as in separately analyzed young-root material (Fig. 2). In plants induced by exposure to 1.5 mM $[NO_3^-]_o$ (Fig. 3), the induction pattern of NO_3^- influx (measured at 1.5 mM $[NO_3^-]_o$) was similar. Influx ranged from a constitutive level of 0.3 μmol g^{-1} h^{-1} to a fully induced value of 1.2 μmol g^{-1} h^{-1}. Maximal fluxes apparently occurred earlier, at d 2, for plants at 1.5 mM than for plants at 200 μM $[NO_3^-]_o$ (cf. Figs. 2 and 3).

Low-Concentration Systems for NO_3^- Uptake

In uninduced seedlings, a saturable NO_3^- influx system was apparent in the concentration range from of 2.5 to 500 μM $[NO_3^-]_o$ (Fig. 4A), and at 1 mM $[NO_3^-]_o$ influx had increased to almost double the saturated rate. The saturable low-concentration phase conformed to Michaelis-Menten kinetics. The kinetic parameters of V_{max} and K_m for this system were determined by several data transformations and a least-squares method (Table I). Estimates for K_m obtained via these methods ranged from 13.6 to 21 μM, whereas V_{max} estimates were between 0.11 to 0.13 μmol g^{-1} h^{-1}.

In seedlings that had been fully induced for NO_3^- influx by exposure of the roots to 100 μM $[NO_3^-]_o$ for 3 d, the low-concentration response of influx was more complex (Fig. 4B). Rather than consisting of a single saturable phase,

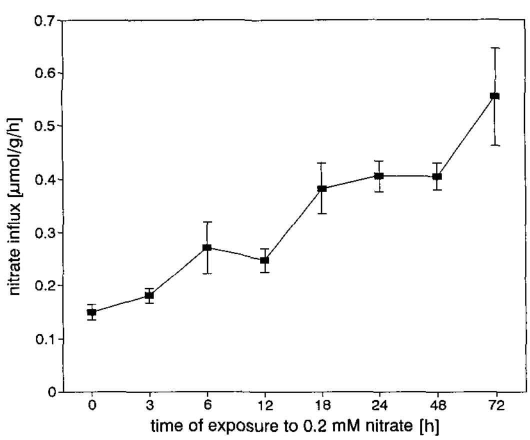

Figure 1. NO_3^- influx into roots of white spruce as a function of short-term exposure to external NO_3^-. Seedlings were cultivated in N-free solutions for 3 weeks and then supplied with 200 μM $[NO_3^-]_o$ for the indicated periods and during the 10-min flux measurements. Data are means ± SE ($n \geq 9$).

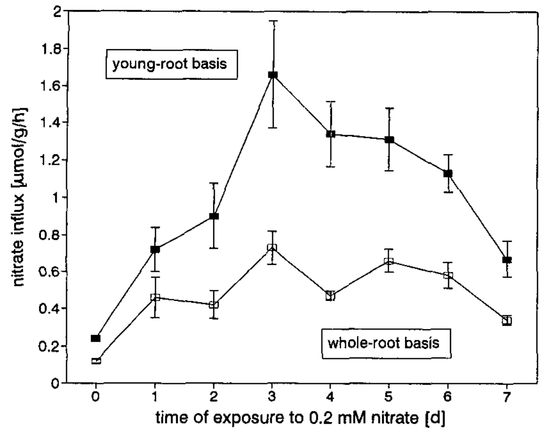

Figure 2. NO_3^- influx into roots of white spruce as a function of longer-term exposure to $[NO_3^-]_o$ at 200 μM (see Fig. 1). Influx was determined both on a young-root basis (top curve) and on a whole-root basis (bottom curve). Data are means ± SE ($n \geq 9$).

low-concentration NO_3^- influx appeared to result from two saturable components, one operating at $[NO_3^-]_o \leq 75$ μM and another operating in the 100 to 750 μM range of $[NO_3^-]_o$. Beyond 750 μM influx again increased beyond the saturated levels. Despite the fact that this biphasic pattern in the low-concentration range was already evident in the influx isotherm, it was confirmed by significance testing of the slopes and y intercepts of the regression lines for the presumed different components in linear transformation plots of the influx data according to Lineweaver-Burk ($P \leq 0.01$ for slopes; $P \leq 0.025$ for intercepts), Eadie-Hofstee ($P \leq 0.005$ for slopes; $P \leq 0.0005$ for intercepts; see Fig. 5), and Hanes-Wolf ($P \leq 0.005$ for slopes; $P \leq 0.05$ for intercepts). Kinetics analyses of the two saturable phases yielded K_m values of 11.1 to 16.8 μM for the first phase and of 98.8 to 153.2 μM for the second phase (Tables II and III). V_{max} estimates were 0.27 to 0.32 μmol g^{-1} h^{-1} for the first component and 0.7 to 0.82 μmol g^{-1} h^{-1} for the second.

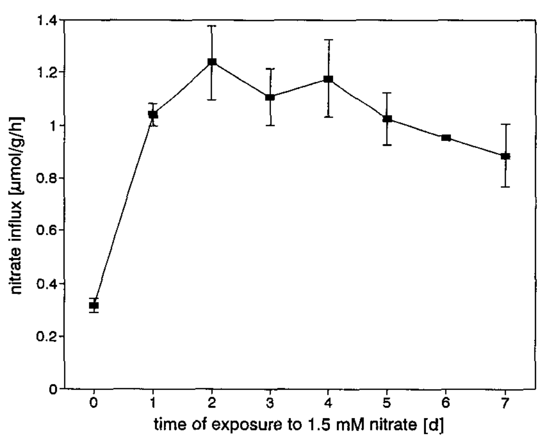

Figure 3. NO_3^- influx into roots of white spruce as a function of time of exposure to $[NO_3^-]_o$ at 1.5 mM (flux measurements were also at 1.5 mM $[NO_3^-]_o$). Data are means ± SE ($n \geq 9$).

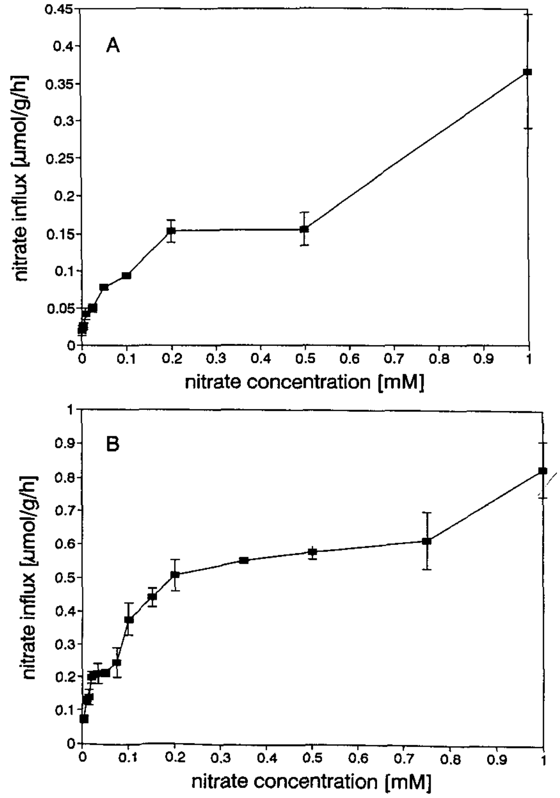

Figure 4. NO_3^- influx into roots of white spruce seedlings as a function of $[NO_3^-]_o$ in the low-concentration range (2.5–1000 μM). Seedlings were either uninduced (A) or induced for NO_3^- uptake by 3-d exposure to 100 μM $[NO_3^-]_o$ (B). Data are means ± SE ($n \geq 9$).

High-Concentration System for NO_3^- Uptake

In both uninduced and induced seedlings an additional linear uptake system operated at higher $[NO_3^-]_o$. It was evident at $[NO_3^-]_o$ of 1 mM in uninduced plants (Fig. 4A) and at $[NO_3^-]_o \geq 750$ μM in plants fully induced for NO_3^- uptake (Fig. 4B). The system was apparently additive to the low-concentration systems. The concentration response of the system between 1 and 50 mM $[NO_3^-]_o$ showed linearity for the entire range ($r^2 = 0.97$; Fig. 6).

Table I. *K_m and V_{max} values for CHATS for NO_3^- in roots of white spruce as estimated by different mathematical methods*

Seedlings were cultivated hydroponically without N for 3 weeks and exposed to external NO_3^- only during the 10-min influx period. An influx isotherm constructed from data pooled from several experiments was used as the basis for calculation of the kinetics parameters (see text).

Calculation Method	K_m	V_{max}	r^2
	µM	*µmol g^{-1} h^{-1}*	
Lineweaver-Burk	13.63	0.11	0.91
Eadie-Hofstee	15.85	0.11	0.81
Hanes-Wolf	21.04	0.13	0.98
Cornish-Bowden	16.96	0.12	–[a]

[a]–, Not based on linear regression.

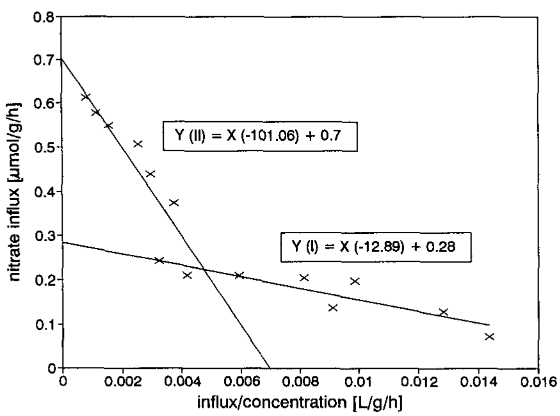

Figure 5. Eadie-Hofstee transformation of the data for induced high-affinity transport of NO_3^- in white spruce (Fig. 4, bottom graph) in the 2.5 to 750 μM range of $[NO_3^-]_o$. Regression lines and linear equations are included for components I and II (see text). The slopes of the two lines ($-K_m$) and the intercepts with the y axis (V_{max}) were significantly different as evaluated by Student's t test ($P \leq 0.005$ for slopes; $P \leq 0.0005$ for intercepts).

DISCUSSION

Time Profile of Transporter Induction

Rates of NO_3^- uptake are considerably enhanced by exposure to $[NO_3^-]_o$, a process usually referred to as NO_3^- induction (Minotti et al., 1969; Goyal and Huffaker, 1986; Behl et al., 1988). Flux increases of at least 5 to 10 times are typically observed (Warner and Huffaker, 1989), but enhancements by as much as 30-fold have been recorded (Siddiqi et al., 1989). Most workers have recorded a lag phase of several hours before induction was apparent (Clarkson, 1986; Warner and Huffaker, 1989), although in some studies a more or less immediate response was found (Tischner et al., 1993). In our experiments with spruce, induction of influx was clearly apparent after 3 h (Fig. 1); however, the induction response was unusually slow in that up to 3 d were required for maximal induction. This was obvious both at the level of young as well as whole root material (Fig. 2). This finding of slow induction kinetics in spruce, which is in agreement with our earlier compartmental analysis results in spruce (Kronzucker et al., 1995b), contrasts sharply with the time required for maximal inductive flux by other species (Glass and Siddiqi, 1995). In barley, however, the time required for induction decreases as $[NO_3^-]_o$ increases (Siddiqi et al., 1989). Similarly, the induction response in spruce appeared to be accelerated at higher $[NO_3^-]_o$ (cf. Figs. 1–3). Nevertheless, spruce remains the slowest responding species so far investigated. This, together with the rather low inductive enhancement factor (only about 5-fold) for V_{max} in the high-affinity range, may be a competitive disadvantage for spruce seedlings compared to nitrophilous species in soil habitats poor in N sources other than NO_3^- (Kronzucker et al., 1995a, 1995b).

Table II. *K_m and V_{max} values for component I of inducible high-affinity influx of NO_3^- into roots of white spruce as estimated by different mathematical methods*

Seedlings were induced for NO_3^- uptake by exposure to 100 μM $[NO_3^-]_o$ for 3 d and were then exposed to various $[NO_3^-]_o$ in concentration dependence experiments (10-min influx periods). See also Table I.

Calculation Method	K_m	V_{max}	r^2
	μM	*μmol g^{-1} h^{-1}*	
Lineweaver-Burk	16.83	0.32	0.97
Eadie-Hofstee	12.89	0.28	0.75
Hanes-Wolf	11.12	0.27	0.97
Cornish-Bowden	14.73	0.3	–[a]

[a]–, Not based on linear regression.

Table III. *K_m and V_{max} values for component II of inducible high-affinity influx of NO_3^- into roots of white spruce as estimated by different mathematical methods (see Tables I and II for details)*

Calculation Method	K_m	V_{max}	r^2
	μM	*μmol g^{-1} h^{-1}*	
Lineweaver-Burk	153.17	0.82	0.9
Eadie-Hofstee	101.06	0.7	0.75
Hanes-Wolf	98.8	0.7	0.99
Cornish-Bowden	112.39	0.73	–[a]

[a]–, Not based on linear regression.

CHATS

Plants that have not been exposed to NO_3^- prior to flux measurement, i.e. are not induced for NO_3^- transport, typically display low rates of NO_3^- uptake. This uptake in the uninduced state has been termed constitutive and is believed to be mediated by a specific saturable HATS (Behl et al., 1988; Warner and Huffaker, 1989; Hole et al., 1990; Siddiqi et al., 1990). Reported K_ms for CHATS in higher plants occur in the range 1 μM (Breteler and Nissen, 1982) to 20 μM (Siddiqi et al., 1990). Our K_m estimates of approximately 15 μM for white spruce are within this range of literature values. Despite the low capacity of the CHATS, it

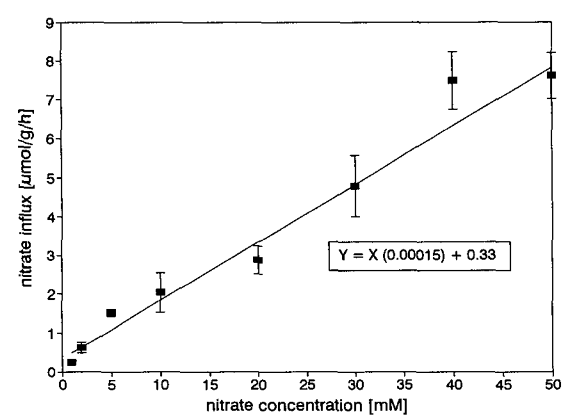

Figure 6. NO_3^- influx into roots of uninduced white spruce seedlings as a function of $[NO_3^-]_o$ in the high-concentration range (1–50 mM). The results of linear regression are included in the graph (r^2 = 0.97). Data means ± SE ($n \geq 9$).

is clearly essential to absorb (catalytic?) NO_3^- in sufficient quantities to induce the IHATS (Glass and Siddiqi, 1995).

IHATS

Most studies of NO_3^- uptake have focused on the inducible NO_3^- transport system operating in the low-concentration range of $[NO_3^-]_o$ (≤1 mM $[NO_3^-]_o$) in induced plants. The system active in that range has typically been found to exhibit saturable kinetics from about 200 to 500 μM $[NO_3^-]_o$. It has been referred to as the IHATS for NO_3^- and has been demonstrated in numerous plant systems (Glass and Siddiqi, 1995). So far, the existence of a saturable IHATS has been demonstrated in Arabidopsis (Doddema and Telkamp, 1979), barley (Rao and Rains, 1976; Bloom, 1985; Lee and Drew, 1986; Konesky et al., 1989; Siddiqi et al., 1990; Aslam et al., 1992), buckwheat (Paulsamy and Chrungoo, 1994), corn (van den Honert and Hooymans, 1955; Neyra and Hageman, 1976; Pace and McClure, 1986; Hole et al., 1990), rice (Youngdahl et al., 1982), ryegrass (Lycklama, 1963), wheat (Goyal and Huffaker, 1986; Botelia et al., 1994), sunflower (Aguera et al., 1990), and squash (Wieneke, 1992). The K_ms reported for IHATS in these species range from 7 to 187 μM (Bloom, 1985; Aslam et al., 1992).

In conifers, kinetic analyses of NO_3^- uptake in the high-affinity or the low-affinity range are scarce. From concentration dependence data obtained through chemical depletion protocols, Peuke and Tischner (1991) calculated a K_m value of 200 μM and a V_{max} of 18 μmol g^{-1} d^{-1} (approximately 0.7–0.8 μmol g^{-1} h^{-1}) for NO_3^- uptake in Norway spruce, and Kamminga-van Wijk and Prins (1993) reported values of 17 μM for K_m and approximately 0.5 to 1 μmol g^{-1} h^{-1} (our calculations) for V_{max} in Douglas fir. Plassard et al. (1994), also using depletion data, communicated a K_m value of 120 μM and a V_{max} of 0.55 μmol g^{-1} h^{-1} for NO_3^- uptake in nonmycorrhizal maritime pine. Since plants in all three studies were exposed to $[NO_3^-]_o$ for some time before uptake rates were determined, the reported values would be subject to the errors described above. Nevertheless, these published values of V_{max} are in reasonably close agreement with our estimates (Table II). The estimates for K_m, however, are not in close agreement. Only Lineweaver-Burk transformations were used in the above studies to provide estimates for the kinetics parameters. Since Lineweaver-Burk plots may yield biased results, in particular regarding K_m (Dowd and Riggs, 1965; Cornish-Bowden and Wharton, 1988), in the present study several mathematical methods were used for the derivation of K_m and V_{max} values. The relatively good agreement between the values obtained by these different methods helped to confirm the validity of the Michaelis-Menten formalism in our data.

The different methods of data transformation establish that NO_3^- influx in induced spruce consisted of two distinct saturable components in the low-concentration range. The possibility that this pattern could arise from different populations of roots cells was ruled out by separately analyzing the kinetics patterns of young, old, and whole root tissues (see "Materials and Methods"). The double-saturation response, albeit with lower V_{max} values in old than in young roots, was apparent in both root tissues (data not shown). Both saturable components conformed to Michaelis-Menten kinetics (Tables II and III), and therefore separate values for K_m and V_{max} are given. Whereas such a pattern of induced influx has usually not been observed (Siddiqi et al., 1989, 1990), the simultaneous operation of a low-K_m and a high-K_m system in the induced high-affinity state has been recently demonstrated through a clearly bimodal Lineweaver-Burk transformation of net uptake data in barley (Aslam et al., 1992). K_m for component I was 7 μM and for component II it was 36 μM. Similar results could be seen in earlier data by Breteler and Nissen (1982) for dwarf bean and Warner and Huffaker (1989) for Steptoe barley. It is interesting that the apparent affinities of both components for NO_3^- were much greater in barley and bean than in spruce, pointing to a relatively poorer adaptation to this N source in the conifer (Kronzucker et al., 1995a).

In our study, all linear transformation methods used confirmed that the assumed differences between the two saturable components were statistically significant (see Figs. 6–8). However, unlike the study by Aslam et al. (1992), the double-saturation pattern of influx was evident even in the isotherms without data transformation (Fig. 4B). It is possible that, because of much larger influx enhancement following induction in cereal species than in spruce (Kronzucker et al., 1995b), the low-K_m component may be hidden in the former but much more clearly visible in the latter. Also, if data resolution in the range of component I is not sufficient, indiscriminate data regression of the entire range may reflect the kinetic parameters of the more dominant component II (Plassard et al., 1994).

It has been argued that the low-K_m component may correspond to the CHATS being expressed simultaneously with the IHATS (Aslam et al., 1992; Glass and Siddiqi, 1995). In agreement with Aslam et al. (1992), our data show that even the low-K_m component of influx appeared to be induced significantly. Although the K_m estimates for CHATS and component I of induced high-affinity influx are very close (approximately 15 μM), suggesting that the transport proteins may be identical, V_{max} was about 3 times as high as the constitutive value after induction. Similarly, Aslam et al. (1992) found an increase in barley from 0.82 μmol g^{-1} h^{-1} for V_{max} in the uninduced state to 3 μmol g^{-1} h^{-1} after induction. Therefore, whereas component II of induced high-affinity influx undoubtedly represents an induction response, component I is also clearly inducible, notwithstanding the fact that it may represent the same transport system earlier identified as CHATS.

LATS

Our results demonstrated that, beyond the saturable high-affinity components at lower $[NO_3^-]_o$, NO_3^- influx across the root plasmalemma of spruce followed a linear pattern at $[NO_3^-]_o$ ≥ 500 to 750 μM. This linear system was present in both uninduced and induced seedlings (data shown only for uninduced seedlings) and appeared to be additive to the high-affinity components, as in other plant systems (Siddiqi et al., 1990; Aslam et al., 1992). In our data (cf. A and B in Fig. 4), the transition from the saturable to the linear phase was visible earlier (at approximately 500 μM $[NO_3^-]_o$) in uninduced plants than in induced plants (at approximately 750 μM $[NO_3^-]_o$). This is in agreement with studies in cereal species (Siddiqi et al., 1990; Aslam et al., 1992).

A dual pattern of NO_3^- uptake (i.e. saturable and linear), as observed in the present study for spruce, has been recorded in several species, including the diatom *Skeletonema costatum* (Serra et al., 1978), *Arabidopsis thaliana* (Doddema and Telkamp, 1979), several varieties of barley (Siddiqi et al., 1990; Aslam et al., 1992), and corn (Pace and McClure, 1986). By contrast, it has been claimed that NO_3^- uptake in spruce is limited to a saturable system and that a linear system is not expressed even at $[NO_3^-]_o$ up to 10 mM (Peuke and Tischner, 1991). Plassard et al. (1994) also reported a lack of substantial increases of NO_3^- uptake rates beyond the saturable low-concentration component in maritime pine. It has to be noted, however, that the studies from which these conclusions have been drawn were based on the measurement of chemical depletion of NO_3^- from solution and that the plants used in these studies were grown in NO_3^--containing media for extended periods. As pointed out earlier, such measurements can provide only estimates of NO_3^- net flux rather than influx. Influx at high $[NO_3^-]_o$ may be obscured by efflux of NO_3^- from the root tissue and by physiological changes occurring in the plants during the extended durations of measurement. Moreover, it is known that the linear LATS responds markedly to tissue N status and that its slope is significantly depressed in plants grown at high compared to low $[NO_3^-]_o$ (Siddiqi et al., 1990). In our white spruce plants, the effect was evident at different stages of induction, i.e. LATS was more pronounced in uninduced plants than in plants previously exposed to $[NO_3^-]_o$ for 3 d. It is conceivable, therefore, that in plants cultivated under conditions of high $[NO_3^-]_o$ LATS may be indistinguishable from the saturation plateau of HATS. However, the present study establishes clearly the presence of a LATS, which under perturbation conditions mediates a linear increase in NO_3^- influx up to 50 mM $[NO_3^-]_o$ (Fig. 6).

ACKNOWLEDGMENTS

Our thanks go to Dr. M. Adam and Mr. P. Culbert at the particle acceleration facility (Tri-University Meson Facility) on the University of British Columbia campus for providing ^{13}N, to Drs. R.D. Guy and S. Silim for providing plant material, and to Dr. M.Y. Wang and Mr. J. Mehroke for essential assistance with isotope experiments. We further wish to extend our thanks to the two anonymous reviewers of this manuscript, whose comments were unusually constructive and helpful.

Received April 21, 1995; accepted June 26, 1995.
Copyright Clearance Center: 0032-0889/95/109/0319/08.

LITERATURE CITED

Aguera E, de la Haba P, Fontes AG, Maldonado JM (1990) Nitrate and nitrite uptake and reduction by intact sunflower plants. Planta **182:** 149–154

Aslam M, Travis RL, Huffaker RC (1992) Comparative kinetics and reciprocal inhibition of nitrate and nitrite uptake in roots of uninduced and induced barley (*Hordeum vulgare* L.) seedlings. Plant Physiol **99:** 1124–1133

Behl R, Tischner R, Raschke K (1988) Induction of a high-capacity nitrate-uptake mechanism in barley roots promoted by nitrate uptake through a constitutive low-capacity mechanism. Planta **176:** 235–240

Bloom AJ (1985) Wild and cultivated barleys show similar affinities for mineral nitrogen. Oecologia **65:** 555–557

Botelia MA, Cerda A, Lips SH (1994) Kinetics of NO_3^- and NH_4^+ uptake by wheat seedlings. Effect of salinity and nitrogen source. J Plant Physiol **144:** 53–57

Breteler H, Nissen P (1982) Effect of exogenous and endogenous nitrate concentration on nitrate utilization by dwarf bean. Plant Physiol **70:** 754–759

Cawse PA (1967) The determination of nitrate in soil solutions by ultraviolet spectrophotometry. Analyst **92:** 311–315

Clarkson DT (1986) Regulation of the absorption and release of nitrate by plant cells. *In* H Lambers, JJ Neeteson, I Stulen, eds, Fundamental, Ecological and Agricultural Aspects of Nitrogen Metabolism in Higher Plants. Martinus Nijhoff, Boston, MA, pp 3–27

Clarkson DT, Lüttge U (1991) II. Mineral nutrition: inducible and repressible nutrient transport systems. Progr Bot **52:** 61–83

Cornish-Bowden A, Wharton CW (1988) Enzyme Kinetics. IRL Press, Oxford, UK

Cram WJ (1968) Compartmentation and exchange of chloride in carrot root tissue. Biochim Biophys Acta **163:** 339–353

Doddema H, Telkamp GP (1979) Uptake of nitrate by mutants of *Arabidopsis thaliana*, disturbed in uptake or reduction of nitrate. II. Kinetics. Physiol Plant **45:** 332–338

Dowd JE, Riggs DS (1965) A comparison of estimates of Michaelis-Menten kinetic constants from various linear transformations. J Biol Chem **240:** 863–869

Glass ADM, Siddiqi MY (1995) Nitrogen absorption in higher plants. *In* HS Srivastava, RP Singh, eds, Nitrogen Nutrition in Higher Plants. Associated Publishers, New Delhi, India, pp 21–55

Goyal SS, Huffaker RC (1986) The uptake of NO_3^-, NO_2^-, and NH_4^+ by intact wheat (*Triticum aestivum*) seedlings. I. Induction and kinetics of transport systems. Plant Physiol **82:** 1051–1056

Hole DJ, Emran AM, Fares Y, Drew MC (1990) Induction of nitrate transport in maize roots, and kinetics of influx, measured with nitrogen-13. Plant Physiol **93:** 642–647

Jackson WA, Flesher D, Hageman RH (1973) Nitrate uptake by dark-grown corn seedlings. Some characteristics of apparent induction. Plant Physiol **51:** 120–127

Kamminga-van Wijk C, Prins HBA (1993) The kinetics of NH_4^+ and NO_3^- uptake by Douglas fir from single N-solutions and from solutions containing both NH_4^+ and NO_3^-. Plant Soil **151:** 91–96

Kamula SA, Peterson CA (1994) The plasmalemma surface area exposed to the soil solution is markedly reduced by maturation of the exodermis and death of the epidermis in onion roots. Plant Cell Environ **7:** 1183–1193

Klobus G, Ward MR, Huffaker RC (1988) Characteristics of injury and recovery of net NO_3^- transport of barley seedlings from treatments of NaCl. Plant Physiol **87:** 878–882

Konesky DW, Siddiqi MY, Glass ADM, Hasiao AI (1989) Genetic differences among barley cultivars and wild oat lines in endogenous seed nutrient levels, initial nitrate uptake rates, and growth in relation to nutrient supply. J Plant Nutr **12:** 9–35

Kramer PJ (1969) Plant and Soil Water Relationships. McGraw-Hill, New York

Kronzucker HJ, Siddiqi MY, Glass ADM (1995a) Compartmentation and flux characteristics of nitrate in spruce. Planta **196:** 674–682

Kronzucker HJ, Glass ADM, Siddiqi MY (1995b) Nitrate induction in spruce: an approach using compartmental analysis. Planta **196:** 683–690

Kronzucker HJ, Siddiqi MY, Glass ADM (1995c) Compartmentation and flux characteristics of ammonium in spruce. Planta **196:** 691–698

Lee RB, Drew MC (1986) Nitrogen-13 studies of nitrate fluxes in barley roots. II. Effect of plant N-status on the kinetic parameters of nitrate influx. J Exp Bot **37:** 1768–1779

Lycklama JC (1963) The absorption of ammonium and nitrate by perennial ryegrass. Acta Bot Neerl **12:** 361–423

McKenzie BE, Peterson CA (1995a) Root browning in *Pinus banksiana* Lamb. and *Eucalyptus pilularis* Sm. I. Anatomy and permeability of the white and tannin zones. Bot Acta **108:** 127–137

McKenzie BE, Peterson CA (1995b) Root browning in *Pinus banksiana* Lamb. and *Eucalyptus pilularis* Sm. II. Anatomy and permeability of the cork zone. Bot Acta **108:** 138–143

Minotti PL, Williams DC, Jackson WA (1969) Nitrate uptake by wheat as influenced by ammonium and other cations. Crop Sci **9:** 9–14

Neyra CA, Hageman RH (1976) Relationship between carbon dioxide, malate and nitrate accumulation and reduction in corn (*Zea mays* L.) seedlings. Plant Physiol **58:** 726–730

Pace GM, McClure PR (1986) Comparison of nitrate uptake kinetic parameters across maize inbred lines. J Plant Nutr **9:** 1095–1111

Paulsamy S, Chrungoo NK (1994) Nitrate uptake in common buckwheat (*Fagopyrum esculentum* Moench): kinetics. Environ Exp Bot **34:** 207–212

Peuke AD, Tischner R (1991) Nitrate uptake and reduction of aseptically cultivated spruce seedlings, *Picea abies* (L.) Karst. J Exp Bot **42:** 723–728

Plassard C, Barry D, Eltrop L, Mousin D (1994) Nitrate uptake in maritime pine (*Pinus pinaster*) and the ectomycorrhizal fungus *Hebeloma cylindrosporum*: effect of ectomycorrhizal symbiosis. Can J Bot **72:** 189–197

Rao KP, Rains DW (1976) Nitrate absorption by barley. I. Kinetics and energetics. Plant Physiol **57:** 55–58

Rüdinger M, Hallgren SW, Steudle E, Schulze E-D (1994) Hydraulic and osmotic properties of spruce roots. J Exp Bot **45:** 1413–1425

Serra JL, Llama MJ, Cadenas E (1978) Nitrate utilization by the diatom *Skeletonema costatum*. I. Kinetics of nitrate uptake. Plant Physiol **62:** 987–990

Siddiqi MY, Glass ADM, Ruth TJ, Fernando M (1989) Studies of the regulation of nitrate influx by barley seedlings using $^{13}NO_3^-$. Plant Physiol **90:** 806–813

Siddiqi MY, Glass ADM, Ruth TJ, Rufty TW (1990) Studies of the uptake of nitrate in barley. I. Kinetics of $^{13}NO_3^-$ influx. Plant Physiol **93:** 1426–1432

Sutton RF, Tinus RW (1983) Root and root system terminology. For Sci Monogr No. 24

Tischner R, Waldeck B, Goyal SS, Rains WD (1993) Effect of nitrate pulses on the nitrate-uptake rate, synthesis of mRNA coding for nitrate reductase, and nitrate-reductase activity in the roots of barley seedlings. Planta **189:** 533–537

van den Honert TH, Hooymans JJM (1955) On the absorption of nitrate by maize in water culture. Acta Bot Neerl **4:** 376–384

Warner RL, Huffaker RC (1989) Nitrate transport is independent of NADH and NAD(P)H nitrate reductases in barley seedlings. Plant Physiol **91:** 947–953

Wieneke J (1992) Nitrate fluxes in squash seedlings measured with ^{13}N. J Plant Nutr **15:** 99–124

Youngdahl LJ, Pacheco R, Street JJ, Vlek PLG (1982) The kinetics of ammonium and nitrate uptake by young rice plants. Plant Soil **69:** 225–232